Suppression of Multiphoton Ionization with Circularly Polarized Coherent Light

P. H. Bucksbaum, M. Bashkansky,[a] R. R. Freeman, and T. J. McIlrath[b]
AT&T Bell Laboratories, Murray Hill, New Jersey 07974

and

L. F. DiMauro
Department of Physics and Astronomy, Louisiana State University, Baton Rouge, Louisiana 70803
(Received 25 February 1986)

Multiphoton ionization in xenon has been studied with 1064-nm circularly polarized coherent light, producing electrons with energies up to 15 eV. A strong suppression of the cross section is observed for electrons below 4 eV, but not for linearly polarized light at the same intensity. We show that if the electrons are emitted in single-step, nonresonant coherent processes, rather than stepwise excitation, the centrifugal potential barrier in the atomic Hamiltonian produces this suppression.

PACS numbers: 32.80.Rm

Amplified mode-locked lasers can produce focusable intensities as high as 10^{15} W/cm^2 where light-field energy densities approach the Coulomb-binding-energy density in atoms. Studies of multiphoton ionization (MPI) in this intensity range reveal a number of dramatic features.[1] Chief among these is above-threshold ionization (ATI), in which electrons are produced not only near the ionization threshold, but at a whole series of energies separated by the photon energy $h\nu$. Several theoretical papers have attempted to explain the qualitative behavior of these higher-order peaks, appealing to either stepwise transitions in the continuum, or direct coherent processes from the ground state.[2]

Experiments reported previously have used linearly polarized light. Here we show that the use of circularly polarized radiation at 1064 nm for MPI in xenon dramatically changes the energy distribution of the final-state electrons, suppressing all electrons from threshold to > 4 eV. Although neither the number of high-energy photoelectrons nor the total ionization rate is significantly reduced, the average photoelectron energy moves much higher. This phenomenon is wavelength dependent; for 532-nm radiation only the first ionization peak is suppressed. A simple model, based on angular momentum absorption and suppression of the overlap with low-energy final states by centrifugal repulsion, agrees well with these observations, and predicts this effect independently from the detailed structure of the atom. Thus the effect should be a general property shared by virtually all atoms. These results indicate that ATI photoelectrons are produced in single-step, nonresonant coherent processes directly from the ground state.

These experiments employ transform-limited 100-ps-duration mode-locked Nd-doped yttrium-aluminum-garnet pulses (1064 nm) or the second harmonic of these pulses (532 nm, 70 ps). The light is focused with a 15-cm lens ($f/10$) to a waist diameter of less than 30 μm for 1064-nm light pulses and less than 16 μm for 532-nm light pulses (less than 3 times the TEM_{00} diffraction limit in both cases). Final polarization is adjusted outside the chamber.

The vacuum chamber houses the interaction region, the electron spectrometer, and the electron detector. The chamber base pressure is maintained at 1×10^{-8} Torr, and xenon gas density is varied by a change of the rate of flow through a leak valve. The spectrometer is a time-of-flight type, consisting of a magnetically shielded, tubular, copper Faraday cage with a 38-cm drift length.

Electrons are detected by microchannel plates which subtend a 3° angle at the source, and are recorded by a transient waveform digitizer with 2-ns resolution. Stray fields limit the overall resolution to approximately 0.03 eV at an energy of 1 eV. A time-of-flight spectrum is recorded for every laser shot, and single electron pulses are discriminated and binned.

Space-charge–induced broadening and shifts are avoided by adjustment of the xenon density to maintain two or fewer detected electrons per laser shot. For low 1064-nm intensities, we find that the ionization rate increases as I^m with $m \approx 10$. Lompre *et al.* have discussed how the measured value of m may deviate from the total number of photons absorbed per atom, as a result of laser spatial and temporal inhomogeneity and jitter.[3] At laser pulse energies above 7 mJ, the intensity dependence changes to $m \approx 1.5$. We interpret this as depletion saturation, which should occur when the ionization rate exceeds the inverse pulse width.

Figure 1(a) is a 10000-shot electron spectrum for MPI in xenon using 1.1-mJ pulses of 532-nm linearly polarized light. The vertical scale is normalized to number of counts per shot, per millitorr of xenon pressure, per millielectronvolt energy bin. The laser polarization is along the detection axis. The MPI electron angular distributions are generally peaked along

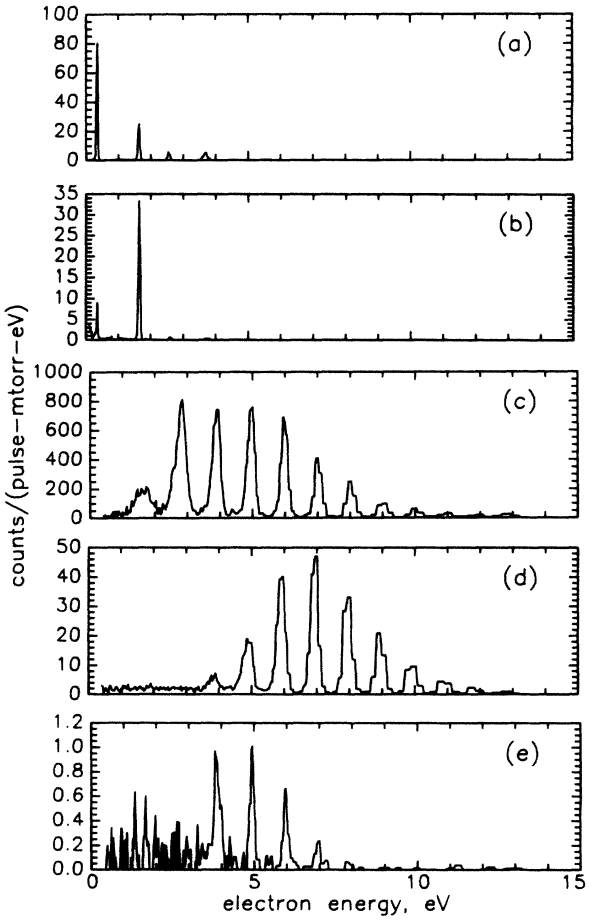

FIG. 1. Photoelectron energy spectrum for (a) 1.1 mJ, 1×10^{-5} Torr, 532 nm, linear polarization; (b) 1.5 mJ, 1×10^{-5} Torr, 532 nm, circular polarization; (c) 11 mJ, 2×10^{-6} Torr, 1064 nm, linear polarization; (d) 11 mJ, 1×10^{-5} Torr, 1064 nm, circular polarization; (e) 6.3 mJ, 1×10^{-5} Torr, 1064 nm, circular polarization. Collection solid angle $\approx 2.5\times10^{-3}$ sr along direction of linear polarization and in plane of circular polarization. Anisotropy of linear-polarization signal enhances collection efficiency by ≥ 12 over circular polarization.

the laser polarization for linearly polarized light. At least six photons must be absorbed in order to ionize xenon, which has series limits of 12.13 and 13.43 eV, corresponding to the $^2P_{3/2}$ and $^2P_{1/2}$ fine-structure levels, respectively, of the $5s^25p^5$ ground configuration of Xe^+. The two lowest-energy peaks in the figure represent six-photon ionization to these two final states. The higher peaks are examples of ATI. Figure 1(b) shows a spectrum at similar intensity, but with circular polarization.

The electron spectra are repeated in Figs. 1(c) and 1(d), but for 1064-nm laser pulses. Eleven photons are required to ionize to the lowest state of Xe^+, and twelve photons to reach the higher $^2P_{1/2}$ state. There is no sign of a peak in the spectrum corresponding to either of these transitions. The lowest-energy spectral feature occurs in the vicinity of ATI processes representing twelve- and thirteen-photon absorption to the two Xe^+ fine-structure states. The relative suppression of the threshold electrons in xenon for linear-polarization MPI has been observed previously.[4] Figure 1(d) is a spectrum taken at the same 1064-nm laser intensity as Fig. 1(c), but with circular polarization. The lowest MPI electron peaks are missing as before, but in addition, the next four ATI peaks in the spectrum are also absent. This striking effect appears to be independent of laser intensity, over a range of at least an order of magnitude. The smaller number of low-energy electrons which were detected are consistent with background. We have repeated these measurements under varying conditions of gas density and laser intensity, but have never succeeded in observing low-energy electron peaks with circularly polarized 1064-nm light.

The disappearance of the low-energy electrons can be explained by a severe reduction of the transition matrix elements for low-energy ATI electron states due to the high orbital angular momentum of the final continuum states. For xenon, absorption of n photons with n units of angular momentum requires transitions into the $L \geq n-1$ continuum. To understand how this suppresses low-energy electrons, consider the transition matrix element M for ATI in atomic hydrogen. The general features of this calculation can be extended easily to ATI transitions in other atoms since the hydrogenic wave functions are good descriptions of high-angular-momentum states of complex atoms. M is given by

$$M=(eE)^n\sum_{i_1}\cdots\sum_{i_{n-1}}\left(\frac{\langle\psi_f|d^+|i_{n-1}\rangle\cdots\langle i_1|d^+|\psi_0\rangle}{\delta E_{n-1}\cdots\delta E_1}\right). \quad (1)$$

In this expression, the wave functions $|i_m\rangle$ represent intermediate states. The initial and final states are $|\psi_0\rangle$ and $|\psi_f\rangle$, respectively, and the detuning associated with the intermediate state $|i_m\rangle$ is $\delta E_i = E_i - E_0 - m\hbar\omega$. E is the electromagnetic field strength. In this high-order nonresonant process one may assume that the energy denominator is effectively constant over the summand, and sum over the numerator alone.[5] Since each intermediate sum is over the complete set of atomic states, the sum over the intermediate states $|i\rangle\langle i|$ is replaced with the identity matrix $|1\rangle\langle 1|$. M then reduces to a single matrix element,

$$M\propto[(eE)^n/(\delta E)^{n-1}]\langle\psi_f|(d^+)^n|\psi_0\rangle, \quad (2)$$

where e is the electron charge, and δE is the average of

the resonance energies. We can study the variation in the spectrum with intensity and wavelength as predicted by the r^n matrix element.

The final state, which must have definite angular momentum of $n\hbar$ for hydrogen, is repelled from the center of the atom by an effective potential for states of definite angular momentum l:

$$V_{\text{eff}}(r) = -\frac{1}{r} + \frac{l(l+1)}{2r^2} \text{ a.u.} \quad (3)$$

The function $r^n\psi_0$, which must overlap the final wave function in the matrix element, has a maximum probability density localized in a region around $r = na_0$, as shown in Fig. 2. Near threshold, the centrifugal barrier excludes the final-state wave function from this region, effectively inhibiting transitions. At higher energies, corresponding to absorption of more photons and more angular momentum, the transition is made to a higher-angular-momentum state with a larger centrifugal barrier. However, because $r^n\psi_0$ is also peaked at larger r for larger n, the overlap integral eventually becomes significant, and MPI turns on.

For circularly polarized 1064-nm multiphoton ionization of hydrogen, this calculation predicts the suppression of electrons below the 5.0-eV peak corresponding to sixteen-photon absorption. For 532-nm light, the suppression only affects the lowest-energy peak. Figure 3 shows the results of the calculation for xenon where the situation is complicated somewhat by the fact that the ion core has P symmetry, and that the ground-state single-particle wave functions for the neutral atom are p states. Nonetheless, taking these differences into account, it is still possible to evaluate the radial integral to determine the qualitative behavior of the ATI spectrum. The final state is given to good approximation by the spherical Bessel function $j_n(kr)$, where k is the wave vector of the outgoing electron. A single value of $E/\delta E$, introduced into Eq. (2), reproduces the intensity distribution of the observed high-energy peaks in the experimental spectra. We arrive at the prediction that the lowest four electron peaks should be suppressed, as shown in Fig. 3.

These estimates neglect the effects of the strong electromagnetic field on the ionization potential and on the free electrons that are produced in MPI. The highly polarizable Rydberg states, the series limits, and the free electrons all undergo sizable shifts in their potential energy as a result of coherent field effects generally referred to as "ponderomotive forces."[6] These impose an extra potential energy, due to the quiver of the electrons in the oscillating field, equal to $e^2 < E^2 > /4m\omega^2$. The observable effects of this ponderomotive-potential term are difficult to calculate in these experiments, because they depend on the strength of the laser at the specific point of ionization, which may not coincide with the most intense part of the pulse. However, there are two important consequences: First, the momentum of the outgoing ionized electron is reduced, and this is reflected in the wave function. Second, the ground-state wave function has different behavior at large r, reflecting the fact that the ionization potential E' (classically, the escape

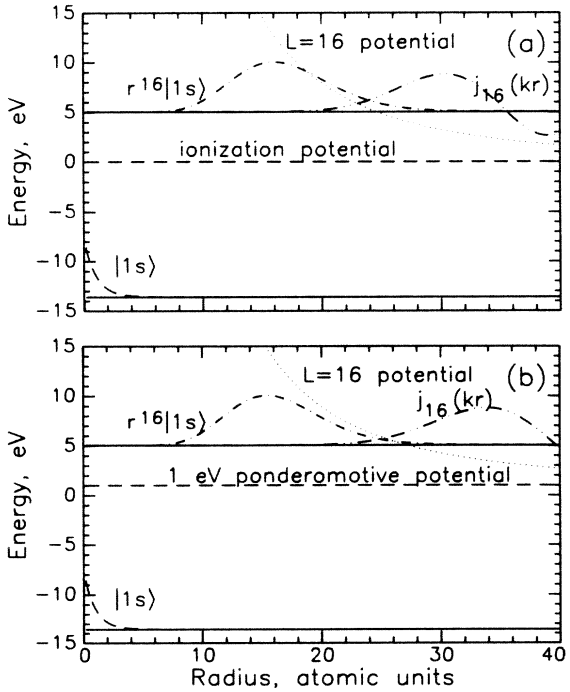

FIG. 2. (a) Effective potential V_{eff} and continuum wave functions $j_{16}(kr)$ for angular momentum $l = 16$ superimposed on $1s$ ground-state wave function and $r^{16}|1s\rangle$ for hydrogen. (b) Same as (a) but with a 1-eV ponderomotive potential.

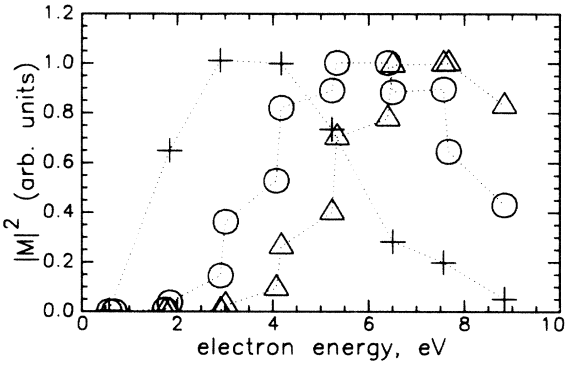

FIG. 3. Variation of $|M|^2$ between the initial $|5p\rangle$ state and final $|E_n\rangle$ continuum state in xenon, corresponding to n-photon absorption. $E_n = nh\nu - E_i$ is the free-electron energy, where E_i is the ionization energy. Angular momentum of continuum state is $l = n + 1$, and E_i includes both Xe^+ final states. Crosses, $h\nu = 532$ nm; circles, $h\nu = 1064$ nm; triangles, $h\nu = 1064$ nm, with a ponderomotive potential of 1 eV.

velocity) has been raised: Specifically,

$$\psi_0(r \to \infty) \propto \exp[-(2mE'/\hbar)^{1/2} r].$$

If ponderomotive energies approaching $h\nu$ are found in the regions of significant ionization, the lowest-energy electron peak will be reduced, as seen in Figs. 2(b) and 3. The data in Fig. 1(e) clearly show an effect consistent with this picture.

In summary, we have observed a nearly complete absence of photoelectrons below 4 eV of kinetic energy in xenon multiphoton ionization using 1064-nm circularly polarized laser light. Linearly polarized light does not exhibit this effect, and the phenomenon is greatly reduced with use of 532-nm radiation. This is due to a centrifugal barrier to ionization which exists if the process is primarily a coherent single step from the ground state. The suppression of lower-order multiphoton ionization should be a general feature of all atoms. Although ponderomotive forces do not play a crucial role in this suppression they do lead to a further reduction in the relative intensity of the lowest visible electron peak at 4 eV.

We wish to acknowledge useful conversations with M. Mittleman, A. Szoke, L. Armstrong, L. Pan, and C. Greene, and technical advice and assistance by D. Schumacher and J. Custer. One of us (T.J.M.) acknowledges the partial support of National Science Foundation Grant No. CPE 81-19250.

Note added.—F. Yergeau, G. Petite, and P. Agostini (private communication) have recently observed low-energy electrons with circularly polarized light (≈ 0.1 our intensity). This shows that at low intensities the $(eEa_0/\delta E)^{2n}$ scaling of $|M|^2$ shifts the spectrum to lower n, as expected. We have set $eEa_0/\delta E \approx 0.2$ in Fig. 3 to match the spectrum above saturation. At this intensity and higher, $\langle r^n \rangle$ dominates the behavior of $|M|^2$.

[a]Also at Physics Department, Columbia University, New York, N.Y. 10027.

[b]On leave from Institute for Physical Science and Technology, University of Maryland, College Park, Md. 20742.

[1]P. Agostini, F. Fabre, G. Mainfray, G. Petite, and N. K. Rahman, Phys. Rev. Lett. **42**, 1127 (1979); P. Kruit, J. Kimman, and M. J. van der Wiel, J. Phys. B **14**, L597 (1981).

[2]M. Edwards, L. Pan, and L. Armstrong, Jr., J. Phys. B. **18**, 1927 (1985); Z. Bialynicka-Birula, J. Phys. B **17**, 3091 (1984); Z. Deng and J. H. Eberly, Phys. Rev. Lett. **53**, 1810 (1984); Z. Deng and J. H. Eberly, J. Opt. Soc. Am. B **2**, 486 (1985); M. H. Mittleman, J. Phys. B **17**, L351 (1984); M. Crance, J. Phys. B **17**, L355 (1984); S.-I Chu and J. Cooper, Phys. Rev. A **32**, 2769 (1985); Y. Gontier, M. Poirier, and M. Trahin, J. Phys. B **13**, 1381 (1980); A. Szoke, J. Phys. B **18**, L427 (1985); K. Rzążewski and R. Grobe, Phys. Rev. Lett. **54**, 1729 (1985).

[3]L. A. Lompre, G. Mainfray, C. Manus, and J. Thebault, Phys. Rev. A **15**, 1604 (1977).

[4]P. Kruit, J. Kimman, H. G. Muller, and M.J. van der Wiel, Phys. Rev. A **28**, 248 (1983); L. A. Lompre, A. L'Huillier, G. Mainfray, and C. Manus, J. Opt. Soc. Am. B **2**, 1906 (1985).

[5]H. B. Bebb and A. Gold, Phys. Rev. **143**, 1 (1966). For circularly polarized light, the nth-order contribution to M includes only states with principal quantum number $\geq n$. These states lie within Ry/n^2 of the ionization energy E_i; for nonresonant processes all of the energy denominators for discrete intermediate states can be approximated by $E_i - n\hbar\omega$. Use of closure on the first $m-1$ contributions reduces M to integrals over the continuum. For the higher-order contributions the intermediate states all have angular momentum greater than $m\hbar$ and the centrifugal barrier reduces the penetration of the wave function so that for low-energy states the radial overlap with the ground state vanishes. The only contribution is from a narrow range of states with sufficient penetration to overlap the initial state. Thus the energy denominator is approximately constant and positive and can be removed from the summand.

[6]T. W. B. Kibble, Phys. Rev. **150**, 1060 (1966); P. Avan, C. Cohen-Tannoudji, J. Dupont-Roc, and C. Fabre, J. Phys. (Paris) **37**, 993 (1976); J. H. Eberly, Prog. Opt. **7**, 359 (1969).